Transient functional blood flow change in the human brain measured non-invasively by diffusing-wave spectroscopy

J. Li,[1] M. Ninck,[1] L. Koban,[2] T. Elbert,[2] J. Kissler,[2] and T. Gisler[1,*]

[1] *Fachbereich Physik, Universität Konstanz, 78457 Konstanz, Germany*
[2] *Fachbereich Psychologie, Universität Konstanz, 78457 Konstanz, Germany*
[*] *Corresponding author: thomas.gisler@uni-konstanz.de*

Compiled June 24, 2008

Multi-speckle diffusing-wave spectroscopy (DWS) is used to measure blood flow transients in the human visual cortex following stimulation by 7.5 Hz full-field and checkerboard flickering. The average decay time $\tau_{\rm d}$ characterizing the decay of the DWS autocorrelation function shows a biphasic behavior: within about 2 s after stimulation onset, $\tau_{\rm d}$ increases rapidly to about 6 % above the baseline value; at later times, $\tau_{\rm d}$ slowly decreases and reaches a steady-state value about 5 % below the baseline value after about 15 s. The initial increase of the DWS signal suggests a transient reduction of the cortical blood flow velocity shortly after stimulation onset. Measurements of this transient response at different positions over the primary visual cortex shows a spatial pattern different from the one measured by EEG.

OCIS codes: (030.6140) Speckle; (170.0170) Medical optics and biotechnology; (170.5270) Photon density waves; (170.5280) Photon migration; (290.1990) Diffusion; (290.1350) Backscattering; (290.4210) Multiple Scattering; (290.7050) Turbid media

In the past few years, near-infrared diffusing-wave spectroscopy (DWS) has developed into a powerful optical method for non-invasively quantifying blood flow in deep tissue [1–5]. DWS (also called diffuse correlation spectroscopy, DCS) measures the temporal autocorrelation function $g^{(2)}(\tau) = \langle I(t)I(t+\tau)\rangle/\langle I(t)\rangle^2$ of the diffusely transmitted intensity $I(t)$ at large distances from the narrow-band light source [6, 7]. Explicitly exploiting multiply scattered light, the technique is sensitive to sub-wavelength scatterer displacements which are, in living tissue, mainly associated with the flow of erythrocytes [8,9]. The strong amplification of blood flow changes by (anatomical or physiological) blood volume variations in perfused tissue makes DWS a very attractive method for the non-invasive monitoring of tumor therapy [10–15].

More recently, near-infrared DWS was used to non-invasively detect functional activity in the human brain through the intact scalp and skull [2,3,5]. Measurements over the somato-motor and the primary visual cortices revealed an accelerated decay of the DWS autocorrelation function during quasi-steady state stimulation, consistent with the enhanced regional blood flow velocity in the activated cortical areas. The initial response of blood flow within the human cortex over time scales too short for reaching the steady state is, on the other hand, not known. In the present Letter we measure transient DWS signals during functional activation of the primary visual cortex, using a novel fiber-based multi-speckle detection setup. We observe an unexpected biphasic response of the DWS signal to full-field and checkerboard flickering suggesting a novel mechanism for rapid adjustment of oxygen supply to rapid stimuli.

Fig. 1(a) schematically shows our multi-speckle DWS setup and the positioning of the optical probes over the visual cortex. Details of the instrument are described in [9]. Briefly, light from a diode laser (Toptica TA-100, $\lambda = 802$ nm) was guided to the scalp by an optical fiber. Diffusely transmitted light was collected by 2 fiber bundles separated 1.5 cm and 3.0 cm from the source. Each receiver fiber was connected to an avalanche photodiode (Perkin-Elmer SPCM-AQ4C). Parallel autocorrelation of the intensity fluctuations from different statistically equivalent speckles, using a 32-channel USB autocorrelator (correlator.com) allows to detect small variations in the DWS signal [5, 9]. In the experiments reported in this Letter, the time resolution for data acquisition was 26.2 ms. At each time, the relative decay time $\tau_{\rm s/b}$ [5] was determined by normalizing the decay time during stimulation $\tau_{\rm d,stimulation}$, by the average baseline value.

In order to detect the time evolution of the DWS signal during stimulation, we measured the stimulus-synchronized average of the relative decay time $\tau_{\rm s/b}$ with a block stimulation paradigm on 5 female subjects (age 21-24). A block measurement consisted of a 20 s baseline period followed by a 60 s stimulation period. During the stimulation period, the subjects stared at a TFT screen (43 cm diagonal at a distance of about 30 cm) flickering at 7.5 Hz; during the baseline period, the subjects fixated a red cross in the center of the dark screen. The optical probes were located about 3.0 cm above the inion [see Fig. 1(b)]. 10 blocks of data were collected from each subject.

During the 60 s stimulation period, the DWS signal shows a clear biphasic pattern (see Fig. 2): within the first 2 s after the onset of the stimulus, the stimulus-synchronized $\tau_{\rm s/b}$ increases rapidly up to about 6% beyond the baseline level, after which it decreases, crossing the baseline at about 6-10 s after the stimulus onset. At still longer times the DWS signal decreases further

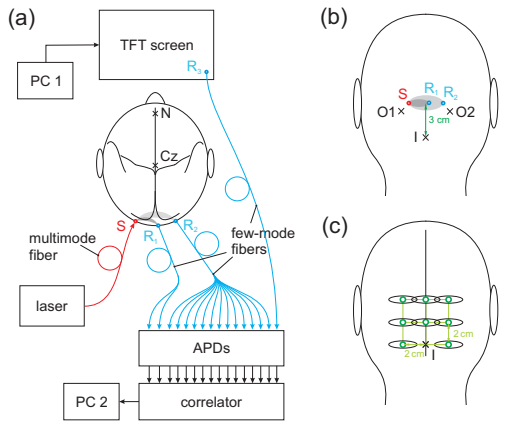

Fig. 1. (a) Experimental setup showing the positioning of the source fiber (S; red circle) and the receiver fiber bundles R_1 and R_2 for the short- and the long-distance probes, respectively (blue circles). Receiver fiber bundles R_1 and R_2 contain 2 and 28 few-mode fibers, respectively (Schaefter+Kirchhoff). Light and dark grey shaded areas indicate the tissue regions probed by short- and the long-distance probe, respectively. I: inion, Cz: vertex, N: nasion. The optical stimulation signal was recorded by receiver R_3 placed directly on the TFT screen. Receiver R_3 is used to detect the flicker signal from the screen in order to precisely determine the onset of each stimulation block. (b) Positioning of the DWS probes over the visual cortex in the time-resolved experiment. (c) Positioning of the DWS probes over the visual cortex in the mapping experiment. The green circles mark the cortical area probed by the long-distance sensors.

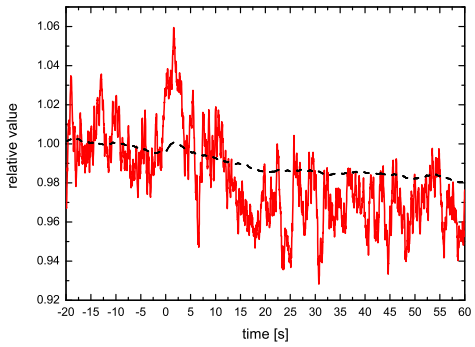

Fig. 2. Stimulus-synchronized average of the relative decay time $\tau_{s/b}$ (red) and of the average photon count rate R (black) measured over the visual cortex with the long-distance sensor as a function of time after onset of visual stimulation ($t = 0\,s$), averaged over 5 subjects. Raw data were smoothed by a sliding average over 1 s.

and, after about 15 s, reaches a saturation value which is about 5% below the baseline level. This saturation value is in agreement with our earlier observation of a reduction of $\tau_{s/b}$ by 3.0-3.8 % during 30 s full-field flickering stimulation [5]. At long times $t > 20\,s$ after onset of stimulation the photon count rate R is reduced below its baseline value by about $1.5 - 2\,\%$, indicating an increase in cortical blood volume which is in line with earlier near-infrared spectroscopy (NIRS) studies [16]. At the short times $0\,s < t \leq 2\,s$ where we observe the large initial increase of $\tau_{s/b}$ the photon count rate R increases slightly by about 0.5 %. However, this increase is statistically not significant in the group average (see below).

The DWS signals and photon count rates from the short-distance receiver R_1, which probes mainly the peripheral hemodynamics in the scalp and in the skull, show similar behavior as the data from the long-distance receiver, however, with strongly reduced amplitude (data not shown), suggesting that the short-distance receiver is partially sensitive to the hemodynamics in the cortex as well.

In the second experiment we focussed on the initial response of the DWS signal during short stimulation blocks. Stimulation blocks consisted of 8.2 s of a checkerboard flickering at 7.5 Hz `Jun Li: how many boxes in x direction, how many in y?` which were separated by baseline intervals of 8-12 s which randomly varied in order to exclude synchronization of peripheral hemodynamics with the stimulus. 10 subjects took part in this experiment (5 male and 5 female, age 19-26). For each subject, 90 blocks of data were recorded.

Fig. 3 shows the group average of the relative DWS signal $\tau_{s/b}$ and count rate $R_{s/b}$ during the 8.2 s stimulation period recorded by the long-distance receiver. The DWS signal shows a statistically significant increase by about 1.18 %. This result is consistent with the time-resolved data shown above where the DWS decay time within the first 8 s after stimulation onset exceeds the baseline value. In contrast, the count rate increases by only 0.15 %; this change is statistically not significant. Similar to the observation in the time-resolved experiment, the DWS signal and the photon count rate recorded by the short-distance receiver parallel the behavior of the long-distance receiver data, albeit with considerably less amplitude.

In order to determine whether the unexpected increase of $\tau_{s/b}$ observed shortly after stimulation onset is due to a particular placement of the optical probe, we performed a mapping experiment on a subject (female, age 26) selected from the second subject group. Selection was based on the high photon count rate available for this subject. Optical probes with 3 cm source-receiver distance were placed at 8 positions over the visual cortex successively, covering an area of $4 \times 4\,cm^2$ directly above the inion [see Fig. 1(c)]. The stimulation protocol was identical with that of the previous experiment.

Fig. 4 shows the maps for the DWS signal (left panel) and the corresponding p-value (right panel) over the visual cortex during the 8.2 s stimulation period. The $\tau_{s/b}$ map shows an increase by 1.0-2.0 % over a large area

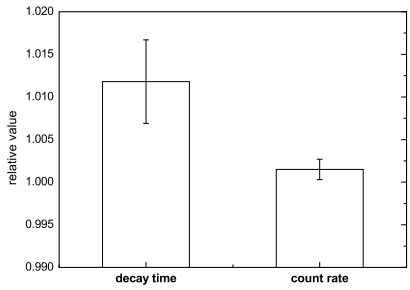

Fig. 3. Group average of the relative decay time $\tau_{s/b}$ and photon count rate $R_{s/b}$ during 8.2 s stimulation with 7.5 Hz checkerboard flickering. Optical probes were placed as shown in Fig. 1(b). Error bars represent the standard deviation for 10 subjects. Student's t-test shows a significant functional increase of the DWS signal ($t(9) = 2.39$, $p = 0.04 < 0.05$), while the count rate signal is not significant ($t(9) = 1.33$, $p = 0.21 > 0.05$).

of the visual cortex, in particular in the left hemisphere where the increase of $\tau_{s/b}$ is as much as 2.0 %. The p-value map shows that the most significant increase of $\tau_{s/b}$ occurs in a strip-like region located 2 cm above the inion with a width of about 1 cm. The observation that this laterally asymmetric pattern is clearly distinct from the symmetric activation pattern measured by EEG (L. Koban et al., unpublished results), and the absence of DWS signals at the frequency of stimulation indicates that the transient DWS signal is hemodynamic in origin.

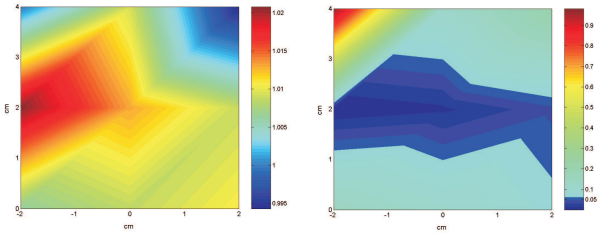

Fig. 4. Map of the relative decay time $\tau_{s/b}$ (left) and the corresponding p-value (right) during 8.2 s checkerboard stimulation over the visual cortex. The position $(0, 0)$ is the inion. In the p-value map, regions of significant changes of $\tau_{s/b}$ (i.e., with $p \leq 0.05$) are marked in blue. Maps are generated by piecewise bilinear interpolation based on the measured values at the 8 sensor positions.

The weak increase of the relative photon count rate $R_{s/b}$ by about 0.5 % for times $0\,\text{s} < t \leq 2\,\text{s}$ suggests a transient reduction of cortical blood volume. We estimate that the corresponding increase in $\tau_{s/b}$ due to the reduction of μ_s' which arises from the reduced erythrocyte concentration in the tissue results in a transient change of $\tau_{s/b}$ by at most 0.5 % [5] which is by more than a decade below the transient DWS signal change. If, on the other hand, we assume Grubb's scaling between changes in relative blood flow and relative blood volume [17], we expect changes of the transient DWS signal of at most 1.5 %, which is about 4 times smaller than the observed DWS signal change. We speculate that the large reduction of flow velocity observed here could serve as a physiological mechanism for increasing the efficiency of oxygen uptake into the cortical tissue shortly after onset of activation.

In conclusion, we have shown that fiber-based multi-speckle diffusing-wave spectroscopy provides access to the functional changes of cortical blood flow in a temporal window which at present is not accessible with any other non-invasive method.

We thank M. Wolf and B. Rockstroh for helpful discussions. This work is funded by the Deutsche Forschungsgemeinschaft (DFG) and the Center for Applied Photonics (CAP) Konstanz.

References

1. D. A. Boas and A. G. Yodh, J. Opt. Soc. Am. A **14**, 192 (1997).
2. T. Durduran, G. Yu, M. G. Burnett, J. A. Detre, J. H. Greenberg, J. Wang, C. Zhou, and A. G. Yodh, Opt. Lett. **29**, 1766 (2004). Non-invasive meas. on humans.
3. J. Li, G. Dietsche, D. Iftime, S. E. Skipetrov, G. Maret, T. Elbert, B. Rockstroh, and T. Gisler, J. Biomed. Opt. **10**, 044002 (2005).
4. J. Li, F. Jaillon, G. Dietsche, G. Maret, and T. Gisler, Opt. Express **14**, 7841 (2006).
5. F. Jaillon, J. Li, G. Dietsche, T. Elbert, and T. Gisler, Opt. Express **15**, 6643 (2007).
6. G. Maret and P. E. Wolf, Z. Phys. B **65**, 409 (1987).
7. D. J. Pine, D. A. Weitz, P. M. Chaikin, and E. Herbolzheimer, Phys. Rev. Lett. **60**, 1134 (1988).
8. G. Yu, T. F. Floyd, T. Durduran, C. Zhou, J. Wang, J. A. Detre, and A. G. Yodh, Opt. Express **15**, 1064 (2007).
9. G. Dietsche, M. Ninck, C. Ortolf, J. Li, F. Jaillon, and T. Gisler, Appl. Opt. **46**, 8506 (2007).
10. C. Menon, G. M. Polin, I. Prabakaran, A. Hsi, C. Cheung, J. P. Culver, J. F. Pingpank, C. S. Sehgal, A. G. Yodh, D. G. Buerk, and D. L. Fraker, Cancer Res. **63**, 7232 (2003). Tumor tissue close to surface.
11. G. Yu, T. Durduran, C. Zhou, H.-W. Wang, M. E. Putt, H. M. Saunders, C. S. Sehgal, E. Glatstein, A. G. Yodh, and T. M. Busch, Clin. Cancer Res. **11**, 3543 (2005).
12. U. Sunar, H. Quon, T. Durduran, J. Zhang, J. Du, C. Zhou, G. Yu, R. Choe, A. Kilger, R. Lustig, L. Loevner, S. Nioka, B. Chance, and A. G. Yodh, J. Biomed. Opt. **11**, 064021 (2006).
13. G. Yu, T. Durduran, C. Zhou, T. C. Zhu, J. C. Finlay, T. M. Busch, S. B. Malkowicz, S. M. Hahn, and A. G. Yodh, Photochem. Photobiol. **82**, 1279 (2006).
14. T. Durduran, R. Choe, G. Yu, C. Zhou, J. C. Tchou, B. J. Czerniecki, and A. G. Yodh, Opt. Lett. **30**, 2915 (2005).
15. G. Yu, T. Durduran, G. Lech, C. Zhou, B. Chance, E. R. Mohler III, and A. G. Yodh, J. Biomed. Opt. **10**, 024027 (2005).

16. M. Wolf, U. Wolf, V. Toronov, A. Michalos, L. A. Paunescu, J. H. Choi, and E. Gratton, NeuroImage **16**, 704 (2002).
17. M. Jones, J. Berwick, D. Johnston, and J. Mayhew, NeuroImage **13**, 1002 (2001).